HHS Public Access

Author manuscript

Cell. Author manuscript; available in PMC 2016 October 22.

Published in final edited form as:

Cell. 2015 October 22; 163(3): 746–758. doi:10.1016/j.cell.2015.09.056.

Engineering a Therapeutic Lectin by Uncoupling Mitogenicity from Antiviral Activity

Michael D. Swanson[1,13,+], **Daniel M. Boudreaux**[1,2,+], **Loïc Salmon**[2,+], **Jeetender Chugh**[2], **Harry C. Winter**[3], **Jennifer L. Meagher**[4], **Sabine André**[5], **Paul V. Murphy**[6], **Stefan Oscarson**[7], **René Roy**[8], **Steven King**[1], **Mark H. Kaplan**[1], **Irwin J. Goldstein**[3], **E. Bart Tarbet**[9], **Brett L. Hurst**[9], **Donald F. Smee**[9], **Cynthia de la Fuente**[10], **Hans-Heinrich Hoffmann**[10], **Yi Xue**[11], **Charles M. Rice**[10], **Dominique Schols**[12], **J. Victor Garcia**[13], **Jeanne A. Stuckey**[4], **Hans-Joachim Gabius**[5], **Hashim M. Al-Hashimi**[2,11,+,*], and **David M. Markovitz**[1,+,*]

[1]Division of Infectious Diseases, Department of Internal Medicine, Program in Immunology, University of Michigan, Ann Arbor, Michigan 48109, USA [2]Department of Biophysics, University of Michigan, Ann Arbor, Michigan 48109, USA [3]Department of Biological Chemistry, University of Michigan, Ann Arbor, Michigan 48109, USA [4]Life Sciences Institute, University of Michigan, Ann Arbor, Michigan 48109, USA [5]Institute of Physiological Chemistry, Faculty of Veterinary Medicine, Ludwig-Maximilians-University Munich, 80539 Munich, Germany [6]School of Chemistry, National University of Ireland, Galway, Ireland [7]Centre for Synthesis and Chemical Biology, University College Dublin, Belfield, Dublin 4, Ireland [8]Department of Chemistry, Université du Québec à Montréal, Montréal, Québec H3C 3P8, Canada [9]Institute for Antiviral Research, Utah State University, Logan, Utah 84322, USA [10]Rockefeller University, New York, New York 10065, USA [11]Department of Biochemistry, Duke University, Durham, North Carolina 27710, USA [12]Laboratory of Virology and Chemotherapy, Rega Institute for Medical Research, University of Leuven, 3000 Leuven, Belgium [13]Division of Infectious Diseases, Department of Medicine and UNC AIDS Center, University of North Carolina, Chapel Hill, North Carolina 27599, USA

Summary

[*]Corresponding authors: David M. Markovitz: dmarkov@umich.edu; Hashim M. Al-Hashimi: ha57@duke.edu.
[+]Equal contribution

Author Contributions

M.D.S. created the H84T mutant, tested its activity against HIV *in vivo* and *in vitro*, assessed mitogenicity, and helped write the manuscript. D.M.B. created the multiple H84 mutants, produced the BanLec to be analyzed by NMR, and ran NMR assays. L.S. performed the N.M.R. studies, along with J.C., determined the NMR assignments, and helped write the manuscript. H.C.W. and I.J.G. performed agglutination assays and ITC. M.H.K. suggested separating mitogenicity from antiviral activity and helped design experiments. P.V.M., S.O., and R.R. designed and synthesized the glycoclusters. S.K. performed antiviral studies and refined production of BanLec. E.B.T., B.L.H., and D.F.S. determined the activity of H84T against WT influenza *in vitro* and *in vivo*. C. d.l.F., H.-H.H., and C.M.R. devised and conducted the HCV experiments. D.S. further determined the activity of H84T against HIV and tested parameters of mitogenicity. J.V.G. helped design and supervised the *in vivo* HIV studies. J.L.M. and J.A.S. performed the X-ray crystallography studies. S.A. and H.-J.G. designed and carried out the studies using glycoclusters and played a major role in writing the manuscript. Y.X. performed the MD simulations. H.M.A-H. directed all structural studies and, along with D.M.M., supervised and integrated the work done by the collaborators and wrote the manuscript.

A key effector route of the Sugar Code involves lectins that exert crucial regulatory controls by targeting distinct cellular glycans. We demonstrate that a single amino acid substitution in a banana lectin, replacing histidine 84 with a threonine, significantly reduces its mitogenicity while preserving its broad-spectrum antiviral potency. X-ray crystallography, NMR spectroscopy, and glycocluster assays reveal that loss of mitogenicity is strongly correlated with loss of pi-pi stacking between aromatic amino acids H84 and Y83, which removes a wall separating two carbohydrate binding sites, thus diminishing multivalent interactions. On the other hand, monovalent interactions and antiviral activity are preserved by retaining other wild-type conformational features and possibly through unique contacts involving the T84 side chain. Through such fine-tuning, target selection and downstream effects of a lectin can be modulated so as to knock down one activity while preserving another, thus providing tools for therapeutics and for understanding the Sugar Code.

Keywords

antiviral; β-prism; glycocluster; lectin; mitogenicity; stacking

Introduction

Protein-carbohydrate interactions play essential roles in many biological processes, including adhesion and growth regulation, infection, and tumor pathogenesis (Gabius, 2015; Solís et al., 2015). Glycan-encoded information can be translated into cellular effects by receptors, termed lectins (Boyd, 1954). These carbohydrate-binding proteins are widely found in nature, have been put to considerable use in many aspects of glycobiology (André et al., 2015; Gabius et al., 2011, 2015), and hold the potential to be used as antiviral agents. By specifically binding to mannosides of the glycans of glycoproteins on the surface of a virus, they can block viral attachment and/or fusion to cells.

Possible clinical applications of lectins suffer from a major drawback, the potential for side effects mediated by lectin-induced mitogenicity (Borrebaeck and Carlson, 1989). If a mitogenic lectin were used topically in an anti-HIV microbicide, it could lead to uncomfortable inflammation, an increase in viral transmission, and even greater HIV replication because of its ability to activate T cells. Given parenterally, a mitogenic lectin could lead to systemic inflammation (Huskens et al., 2008). To date, it has remained entirely unclear whether mitogenicity and antiviral activity are dissectible in a given lectin.

We set out to rationally engineer a plant lectin isolated from the fruit of bananas (*Musa acuminata*, BanLec) (Singh et al., 2014), so as to eliminate its mitogenicity while retaining its potent antiviral activity. BanLec is a member of the mannose-specific jacalin-related lectin (mJRL) group that functions as a potent T-cell mitogen (Singh et al., 2014). It forms a dimer with two carbohydrate-binding sites (CBS I and CBS II) in each protein subunit (Meagher et al., 2005; Singh et al., 2005). BanLec avidly associates with high-mannose-type N-glycans on the HIV-1 envelope and can thus block viral entry into cells (Swanson et al., 2010; Ferir et al., 2011). Here, we show that a mutation within the sugar-binding site in BanLec makes it possible to significantly decrease mitogenic activity without compromising

antiviral activity against HIV, hepatitis C virus (HCV), and influenza virus, all of which have high-mannose-type N-glycans on their surfaces. This new form of BanLec thus has the potential to be used as a broad-spectrum antiviral agent, something that is presently not available in the clinic. Further, we detail the molecular basis for separating these two distinct activities of the lectin. Our results provide proof of the feasibility of re-engineering target specificity and activity of a lectin, an approach that will greatly help clarify how lectins read and transmit information through the Sugar Code, the biochemical platform that turns complex, sugar-encoded information into a broad spectrum of biological activities (Gabius et al., 2011; Murphy et al., 2013; Solís et al., 2015).

Results

The antiviral and mitogenic activities of BanLec can be uncoupled through substitution of a single amino acid

The BanLec cDNA was cloned, and the recombinant protein containing a 6x His-tag, with the sequence LEHHHHHH, expressed in *E. coli*. Unless stated otherwise, all of the BanLec proteins utilized in this study are recombinant versions containing a His-tag. The recombinant His-tagged version of BanLec maintains mannose-binding properties as measured by isothermal titration calorimetry (ITC) (see discussion below) and anti-HIV activity (Figure S1). Natural BanLec is a mitogen (Gavrovic-Jankulovic et al., 2008), and we confirmed this finding with the recombinant version by exposing peripheral blood lymphocytes (PBL) to the lectin for three days and measuring incorporation of BrdU (Figure 1A and Figure S1).

To pinpoint potentially promising sites for mutational engineering, we examined crystal structures of the β-prism I structure, which is characteristic for the JRL family (Meagher et al., 2005; Singh et al., 2005). This fold consists of three Greek Key structures composed of β-strands; distinct loops found in the Greek Keys play a role in carbohydrate binding. The first and second Greek Keys include the JRL consensus motif GXXXD for sugar binding, and when mutations were introduced into these Greek Keys they abolished the mitogenic activity (as seen with the D133G mutant shown in Figure 1A), but also resulted in a loss of almost all anti-HIV activity (data not shown). The third Greek Key varies among JRL members in length and sequence, and is thought to play a role in binding glycan structures beyond simple saccharides (Nakamura-Tsuruta et al., 2008). H84 is part of this third loop, known to be involved in binding the second sugar moiety in α1,6-dimannosides (Singh et al., 2005). Therefore, we reasoned that altering this amino acid might result in a change in binding characteristics that would affect the lectin's mitogenic and antiviral activities differentially.

Several H84 BanLec mutants were constructed (see further discussion below), and one variant, H84T, in which the histidine is replaced by a threonine, was found not to stimulate the proliferation of lymphocytes at concentrations up to 1 μM (Figure 1A). While increased cell surface expression of the activation marker CD69 was observed for BanLec-treated $CD4^+$ peripheral blood mononuclear cells (PBMC), the H84T variant induced very little stimulation of this same marker (Figure 1B). Moreover, wild-type (WT) BanLec consistently caused a large increase in the induction of cytokines from the PBMC of

multiple individual donors, whereas the response to H84T was markedly reduced (Figure 1C). Thus, H84T, unlike naturally- occurring and WT recombinant BanLec, is minimally mitogenic when tested by three independent methods on the peripheral blood cells of multiple different donors.

In contrast to its loss of mitogenicity, the H84T variant had an IC_{50}-value against HIV in the low nanomolar range and was equally effective at inhibiting a wide range of HIV isolates as was WT BanLec, including multiple clinical isolates from different clades of Group M, a Group O clinical isolate, and a clinical isolate of HIV-2 (Table 1). Of note, a number of the isolates that were susceptible to H84T at low nanomolar concentrations required higher concentrations of the anti-HIV lectin Microvirin and/or were very difficult to inhibit with 2G12, a classic neutralizing anti-HIV monoclonal antibody (Table 1). Recombinant H84T without the His-tag showed very similar anti-HIV activity (data not shown).

To determine the capacity of H84T BanLec to prevent mucosal HIV transmission, we utilized the bone marrow-liver-thymus (BLT) humanized mouse model (Wahl et al., 2012). H84T or PBS (the carrier) were topically applied to the vagina prior to challenge with HIV-$1_{JR\text{-}CSF}$. Fifty percent of the mice treated vaginally with PBS only became infected, as determined by the presence of viral RNA in the plasma. In contrast, none of the mice treated topically with H84T showed detectable levels of viral RNA in the plasma during the course of the experiment ($p=0.0359$; Figure 2A).

The antiviral efficacy of H84T was further evaluated against another important pathogenic virus that presents oligomannoside chains on its surface proteins, hepatitis C virus (HCV; (Goffard et al., 2005)). An intergenotypic HCVcc reporter virus, i.e. BiGluc-Con1/Jc1, was tested in Huh-7.5 cells (Figure S2) (Reyes-del Valle et al., 2012). The addition of H84T to the inoculum decreased HCV in a dose-dependent manner and to levels comparable to inhibition by CD81 antibody, a positive control that blocks the cellular receptor for HCV (Figure S2A and data not shown). Co-incubation of virus inoculum with the BanLec derivative D133G/38A which, similar to the D133G mutant (Figure 1A) is inactive, was found not to decrease viral replication (Figure S2B). At the EC_{90} concentration (determined in Huh-7.5 cells), H84T also reduced HCV replication to levels similar to neutralizing E2 antibody in a primary human fetal liver culture (data not shown). Finally, to determine if the H84T-specific reduction of HCV was due to inhibition of viral RNA replication, the effect of H84T BanLec was monitored in Huh-7.5 CD81 knockdown cells ($CD81^{lo}$; Figure S2C). In this single-cycle assay, H84T decreased HCV replication over time in the control cell background only, further supporting the hypothesis that H84T inhibits viral replication at entry (receptor binding, membrane fusion), consistent with what we previously observed with WT BanLec against HIV (Swanson et al., 2010).

Glycosylation sites on the HCV E1 and E2 envelope proteins are highly conserved across genotypes (Goffard et al., 2005). Utilizing a panel of chimeric *Gaussia* luciferase reporter viruses, in which the structural region (core-NS2) was encoded by differing genotypes, H84T was observed to decrease HCV replication in a dose-dependent manner (Figure 2, B–J; Table S1). H84T BanLec thus appears to be a pan-genotypic inhibitor of HCV infection.

The hemagglutinin of influenza A viruses bears high-mannose-type N-glycans that are susceptible to host lectins (Ng et al., 2012). In studies employing a retroviral core pseudotyped with the hemagglutinins of the 1918 H1N1 and the H5N1 avian pandemic influenza viruses, WT and H84T BanLec were both very active and equally inhibitory (Figure 2K, L).

We next found that H84T BanLec is very active against multiple WT strains of influenza A tested in MDCK cells in tissue culture. Significant activity was seen against A/California/04/2009 (H1N1 pandemic strain), California /07/2009 (H1N1 pandemic strain), A/New York/18/2009 (H1N1 pandemic strain), and Perth/16/2009 (H3N2), with EC_{50} values of 1–4 μg/mL versus H1H1 virus and 0.06–0.1 versus H3N2 virus. A mutant form of BanLec that does not bind mannose, D133G/D38A, had no activity, excluding carbohydrate-independent effects. Importantly, significant activity was also seen with H84T against the Duck/MN/1525/81 H5N1 avian strain (EC_{50} of 5–11 μg/mL), confirming our results obtained with pseudotyped virus (Figure 2L). Finally, as some mouse-adapted strains of influenza lack mannose on their hemagglutinin (Smee et al., 2008), we tested an H1N1 (A/WSN/1933) isolate previously shown to be inhibited by mannose-binding proteins for its sensitivity to our new agent. H84T was indeed quite active against this H1N1 strain, which causes disease in mice. Most importantly, we found that intranasal (IN) H84T BanLec, first given four hours after IN viral challenge, effectively blocks influenza infection in the mouse model (Figure 2M). Taken together, studies with pseudotyped virus, WT virus in tissue culture, and a mouse model of influenza demonstrate significant activity of H84T against multiple strains of influenza.

H84T BanLec is less active in multivalent interactions

To begin to delineate the basis for the H84T mutant protein's markedly decreased mitogenic and pro-inflammatory activity, while yet maintaining its potent antiviral capacity, binding properties of H84T and WT BanLec to monovalent sugars in solution were compared. The association constants (K_a) measured using isothermal titration calorimetry (ITC) for binding to methyl α-*D*-mannopyranoside were similar for recombinant His-tagged WT (383 mM^{-1}) and H84T (353 mM^{-1}), and were consistent with previous measurements for naturally-occurring BanLec (333 mM^{-1}) (Mo et al., 2001; Winter et al., 2005). Interestingly, slightly weaker affinities were observed for H84T as compared to WT when analyzing binding to dimannoside (300 vs. 227 mM^{-1} for WT and H84T, respectively) (Table S2).

As mitogenicity involves cross-linking of distinct counter receptors on cell surfaces that trigger outside-in signaling, the loss of mitogenicity seen with H84T and its slightly diminished binding affinity for disaccharides compared to monosaccharides suggested that the biological differences between the two proteins might arise due to differences in their binding properties to more complex glycans. A simple assay that provides insights into binding to cell surface glycans and cross-linking activity (here in *trans*, that is between cells) is measuring lectin-induced aggregate formation of erythrocytes. The minimal concentrations for agglutination were found to be significantly different, i.e. at 3 μg/mL and 437 μg/mL for WT and H84T, respectively (Table S2). This result reveals a marked

disparity in building stable aggregates based on more than monovalent interactions with cell surface mannosides.

Synthetic glycoclusters are excellent tools, which range in size from bivalent compounds to glycodendrimersomes (Murphy et al., 2013; Solís et al., 2015), so their locally increased density of ligands will trace a change in the interaction/association profile when testing WT and variant proteins under identical conditions. The association of a lectin with a ligand-bearing surface is sensitive to the presence of haptenic sugar, and its presentation in local clusters can enhance its inhibitory capacity. Mimicking the natural display of high-affinity ligands, synthetic glycoconjugates (carbohydrates attached to a scaffold enabling oligo- to polyvalency) thus are able to interfere with lectin binding, ligand-presenting surfaces in quantitative terms. The design of glycoclusters and the determination of their inhibitory activity on lectin binding (to glycoproteins or to a cell), measured as the inhibitory concentration (IC) at which the extent of lectin binding to a glycoligand is reduced by 50% (IC_{50}-value), provide a measure of the avidity of a lectin for multivalent associations. In total, we tested a panel of 11 bi- to dodecavalent glycoclusters systematically in titrations in two types of assay, one biochemical and one cellular. In both cases, the mannose-specific lectin concanavalin A was used as positive control, and lectin binding to the glycan-presenting matrix was ascertained to be saturable and dependent on carbohydrate presence.

First, we established a surface rich in presentation of mannose residues. A neoglycoprotein (a conjugate of albumin and mannose derivatives) was adsorbed to the plastic surface of microtiter plate wells, building the matrix for letting the biotinylated lectins dock. Surface-associated label was then quantitatively assessed spectrophotometrically. Titrations of the extent of binding with increasing amounts of inhibitor were performed to determine the IC_{50}-value; the glycoclusters (Figure 3A) were individually tested. As can be seen in the example shown in Figure 3B, these experiments allowed us to determine IC_{50}-values as a measure for sensitivity of lectin binding in the presence of inhibitors. Binding of the H84T mutant was found to be much more susceptible to glycocluster inhibition than was surface contact formation of the WT BanLec, consistent with the lower cross-linking capacity in hemagglutination (Table S2, Table S3).

To confirm the above and increase the biological relevance of the findings, we proceeded to monitor cell binding, using the surface of cultured cells as a platform for contact of the labeled lectins. Tested under identical conditions, WT reacted more strongly with cells than did H84T (Figure 3C a,b). In addition to testing the physiologic glycome profile on the cells, we increased the level of lectin-reactive high-mannose-type N-glycans by treating the cells with the α-mannosidase I inhibitor 1-deoxymannojirimycin. Enhanced binding of both proteins was seen (Figure 3C c,d), with the difference in mean fluorescence intensity between H84T and WT being maintained. Thus, increased ligand availability did not reduce the relative difference between H84T and WT proteins. Glycocluster testing on cells, for example the tetravalent compound **11** (Figure 3C e,f), fully confirmed the differential sensitivity seen in the solid-phase assays. These results are completely consistent with the decreased capacity for H84T BanLec to agglutinate erythrocytes, and further confirm that H84T and WT differentially interact with multivalent surfaces, but not with the monosaccharide.

High resolution X-ray structures reveal loss of pi-pi stacking between Y83 and H84 and an altered sugar contact profile in H84T

To examine the structural basis for the difference in carbohydrate-binding modes between WT and H84T, we determined the crystal structures of the recombinant proteins both in the absence and presence of dimannoside (M2) (Figure 4). The X-ray structure of recombinant WT BanLec was very similar to its naturally-occurring, purified counterpart (Meagher et al., 2005), consistent with the similar biological activities of the two proteins. The monomer forms a β-prism I fold containing three Greek Key motifs with 3-fold symmetry and two carbohydrate binding sites (CBS I and II). CBS I consists of loops on the top of the first Greek Key; CBS II sits on the top of the second Greek Key. The two binding sites are separated by a loop (residues 83–88) within the third Greek Key (Figure 4A), which has been suggested to be an important determinant of carbohydrate binding specificity (Meagher et al., 2005); H84 is within this loop. It is worth noting that glycerol units were observed in the different binding sites of the WT protein.

Both recombinant His-tagged proteins (WT and H84T) and the WT from bananas form a dimeric structure with interface between β-strand 1 (residues 4–10), β-strand 10 (residues 110–118) and two C-terminal residues (E140 and P141) from each monomer resulting in a quasi eight-stranded β-sandwich structure. The presence of the C-terminal His-tag on recombinant WT and H84T did not alter the dimer interface nor did its presence disrupt the non-biological asymmetric tetramer that formed due to crystal packing in all the reported BanLec crystals.

Apo WT and H84T form very similar structures as indicated by an overall RMSD of 0.26 Å. Nevertheless, there are significant differences in and around the site of mutation. In WT, H84 stacks on Y83 to form a pi-pi stacking interaction that directs both residues toward CBS II, resulting in a “wall” that separates the two CBS (Figure 4B). In sharp contrast, in H84T, no pi-pi stacking can occur (Figure 4C). Instead, the threonine side chain points towards CBS I (Figure 4C). In WT, the H84/Y83 stack prevents the side chain of residue 84 from pointing towards the CBS I.

The X-ray structures of WT and H84T bound to a dimannoside (M2) feature two dimers in the asymmetric unit forming a non-biological asymmetric tetramer, and four sets of CBS each bound to a dimannoside molecule. The position of the first mannose moiety of M2 is well resolved in the electron density maps of CBS I and II of both proteins, suggesting that it is tightly bound to both structures (Figure 4B, C and Figure S3). In CBS I of the WT and H84T, there are five hydrogen bonds (H-bonds) between each protein and the first mannose moiety, involving OD1 and OD2 of D133 and the backbone N of G15, K130, and F131. In CBS II, there are six H-bonds stabilizing the position of the saccharide, which include side chain atoms OD1 and OD2, of D38 and the backbone N of N35, V36 and G60.

The main difference in ligand binding between the proteins involves the second mannose moiety that is more accessible to solvent and residue 84. This second mannose moiety gives visible electron density in CBS I for three out of four chains of the WT protein and all four chains of the H84T protein, but is present in the CBS II for only one H84T chain. For the CBS I site, each protein makes one H-bond with the second mannose moiety. In WT, the

H84 side chain does not engage in H-bonds with the second mannose moiety in the CBS I pocket (Figure 4B), while in H84T, the side chain of T84 swings into the CBS I pocket to form a H-bond with this O1 hydroxyl oxygen of the sugar (Figure 4C). The existence of pi-pi stacking locks the imidazole ring of H84 towards the CBS II and its loss in H84T allows for this reorientation towards the CBS I. Thus, although the global structures of WT and H84T are not markedly different, the loss of pi-pi stacking alters the carbohydrate-protein contacts and topological presentation of the carbohydrate-binding site, potentially explaining the difference in their biological behavior.

NMR spectroscopy and molecular dynamics (MD) simulations reveal differences in the structures of WT and H84T BanLec

We used solution-state NMR spectroscopy to further delineate any differences between WT and H84T. NMR spectra showing a single set of resonances for the monomeric subunit are consistent with both WT and H84T forming symmetric oligomers. However, both proteins exhibited a tendency to aggregate over time and this precluded application of multidimensional NMR experiments for resonance assignments (Sattler et al., 1999). Although BanLec is a dimer in solution at physiological pH (Khan, et al., 2013), the X-ray structures reveal the possibility of BanLec forming asymmetric tetramers, therefore it is probable that the high protein concentration used in NMR promotes the formation of higher-order aggregates. To reduce this tendency we introduced two mutations: Y46K to disrupt the protein-protein interactions of the tetramer and V66D to increase protein hydrophilicity and to disrupt an additional crystal packing site. The resulting Y46K/V66D mutants of WT and H84T indeed formed stable dimers as judged by ^{15}N NMR spin relaxation measurements (see below) and resulted in spectra very similar to those of BanLec without the Y46K/V66D mutations, with the differences primarily localized around the mutation site (Figures S4A and S5). The double-mutant version of the WT was used to obtain assignments, which were then used to assign its H84T counterpart and the corresponding BanLec proteins lacking the double mutation (Figures S4, S5, and S6). In agreement with the crystal structures, we observed significant overlap when comparing the 2D ^{15}N-^{1}H HSQC spectra of WT and H84T, indicating that the two proteins adopt a similar fold (Figure 5A). However, significant differences in chemical shifts were observed in the third Greek Key, indicating that the H84T mutation does affect the structural and/or dynamics properties at this site.

The chemical shift differences between WT and H84T span the entire ligand recognition loop (residues 83–88), which plays important roles in determining the carbohydrate-binding specificity (Figures 5B and S4B). The mutation may broadly affect the conformation of this loop, possibly due to loss of pi-pi stacking as observed in the X-ray structure. We did not observe significant differences in the ^{15}N NMR spin relaxation rates (Palmer, 2004) for these and other sites, indicating that WT and H84T have similar dynamics at the picosecond to nanosecond time scales as well as similar oligomerization states (Figure S7A). This is consistent with the similar dynamics observed for WT and H84T using conventional molecular dynamics (MD) simulations (Figure S7B). However, accelerated MD simulations (Markwick and McCammon, 2011), which can probe slower motions, showed higher flexibility in the ligand recognition loop (83–87) in H84T as compared to the WT protein, consistent with loss of stabilizing pi-pi stacking interactions (Figure 5E).

Next, we performed NMR chemical shift titrations to investigate the interaction between WT H84T mutant with di- and pentamannosides in solution. The addition of dimannose to WT and H84T or pentamannose to their Y46K/V66D mutant versions resulted in significant chemical shift perturbations or broadening of resonances for residues in and around the sugar-binding pocket defined by the X-ray structure (Figures 5C and S4C, D). In all cases, several resonances from residues involved in sugar binding disappear, e.g. K130 and F131, probably due to exchange broadening (Palmer, 2004). While the sites that experience chemical shift perturbations are very similar between WT and H84T, the perturbations are slightly larger for H84T and differ in direction, particularly for the recognition loop and when binding to pentamannose (Figure 5D and S4C, D). Interestingly, the pentamanose-induced perturbations at 84, 85, and 86 tend to diminish the differences at these sites observed in the absence of sugar, suggesting that sugar-binding stabilizes a more similar backbone conformation for these sites (Figure S4E, F). Overall, these data suggest a greater degree of conformational reorganization upon sugar binding in H84T as compared to WT and different sugar-binding modes for the two proteins, consistent with the X-ray structure.

Correlation between of Y83-H84 stacking, NMR chemical shifts, mitogenicity, and antiviral activity

To further explore the correlation between Y83-H84 stacking, BanLec conformation, and biological activity, we systematically substituted H84 with amino acids that have different abilities to engage in stacking interactions and then examined the consequence on both NMR spectra and biological activity. A panel of ten H84 BanLec mutants was constructed, systematically replacing the imidazole ring with other aromatic structures or with ionic, polar, or aliphatic groups, and even a hydrogen atom in H84G. These studies employed the version of BanLec without the double Y46K/V66D mutation. Replacing H84 with the aromatic residues tryptophan (H84W), tyrosine (H84Y), and phenylalanine (H84F), which can maintain favorable stacking interactions, had minimal effects on mitogenicity and anti-HIV activity (Figure 6A, B). In contrast, replacement of the imidazole by ionic, polar, or aliphatic side chains, including substitutions by the amino acids lysine (H84K), aspartic acid (H84D), glutamic acid (H84E), glutamine (H84Q) and leucine (H84L), resulted in marked loss of both mitogenicity and anti-HIV activity (Figure 6A, B). Only a single mutation (H84G) in this panel of protein variants yielded a reasonably similar but smaller drop in mitogenicity as did H84T while preserving some antiviral HIV activity.

NMR spectra of the different mutants yielded excellent overall overlap, indicating that they all adopt a similar protein fold. The differences relative to WT protein were concentrated in the third Greek Key (83–87) (Figure 6C). Further analysis of these differences yielded an interesting trend for several residues; for A86, the resonances observed in all the mutants fall roughly along a straight line. Similar behaviors, too, were observed for V87 and V88, though the magnitude of the change is smaller and more difficult to resolve due to spectral overlap. Furthermore, mutants with aromatic residues (H84F, H84W, and H84Y) that can support pi-pi stacking between residues 83–84 and that have higher mitogenicity and anti-HIV activity have A86 resonance clustering upfield along the line as compared to other mutants that disrupt pi-pi stacking and have lower mitogenicity and reduced anti-HIV activity (Figure 6). Interestingly, in H84G, which exhibits mitogenicity, A86 also clusters

upfield with the other mitogenic mutants despite disruption of pi-pi stacking. A simple explanation is that BanLec exists in rapid dynamic equilibrium between two states and that the mutations differentially shift the relative population of the two states, with A86, situated on the opposite side of the third Greek Key loop relative to 84, acting as a reporter for this equilibrium shift. For V87 and V88, such trends are more difficult to discern, but clearly resonances cluster depending on whether aromatic or non-aromatic residues are used in the substitution. These two residues constitute the back part of the third Greek Key loop. These results suggest that the mutants with aromatic residues maintain pi-pi stacking interactions between amino acids 83 and 84 (Figure 5F).

Unlike other mutants, H84T retains antiviral activity despite the loss of mitogenicity. Interestingly, in H84T, the A86 resonance presents intermediate NMR characteristics between aromatic and non-aromatic mutants, whereas V87 and V88 cluster with non-aromatic residues. Additionally, in H84T G85 presents a very distinct signature, shared only with the H84G, which also retains some antiviral activity, indicating that the two mutants share some unique conformational properties. This suggests that the third Greek Key loop in the H84T mutant uniquely combines conformational attributes of aromatic and non-aromatic mutants.

Molecular basis for separating two activities of BanLec

Both mitogenicity and antiviral activities of BanLec require association with N-glycans, and so most mutations that block mitogenicity also abolish antiviral activity (Figures 1A and 6). Unlike other mutants, H84T retains high antiviral activity, which requires the capacity to home in on viral glycoproteins with sufficient affinity. This is achieved despite disrupting pi-pi Y83-H84 stacking, which is important for sugar binding, possibly due to compensatory interactions between the side chain of T84 and the sugar and retention of WT-like conformational properties.

In contrast, mitogenicity requires the ability to cross-link cognate binding partners, beyond a simple association. Our data suggest that the loss of 83–84 stacking decreases this capacity in H84T and other mutants both due to slightly reduced sugar-binding affinity (and possibly altered sugar binding specificity) and also due to disruption of the wall that helps create two independent sugar-binding sites, each capable of interacting with a distinct glycan molecule (Figure 5F, left). Rather, in H84T, T84 rotates away from CBS II to interact with sugars in CBS I, effectively mixing recognition elements in the two binding sites (Figure 5F, right). This more open binding pocket may make it more likely for the same glycan molecule to simultaneously interact with the two sugar binding sites and/or binding at one site may engage elements from the second site, resulting in weaker binding affinity for a second glycan molecule (Figure 5F, right). This makes it less likely for H84T to simultaneously interact with multiple glycan molecules as required for mitogenicity.

Discussion

The Sugar Code underlies a key biological route of information transfer by which cell-to-cell interactions and cell signaling is orchestrated. Indeed, sugars can be considered the third type of biological alphabet, along with nucleotides and amino acids (Murphy et al., 2013).

The receptors for glycans (lectins) are endowed with the capacity to target distinct counterreceptors by their structure and topological mode of presentation (Gabius et al., 2015). In doing so, lectins can play a vital role in regulating biological processes such as cell growth and the immune response, and also serve as tools for studying structural aspects of glycobiology (Kaltner and Gabius, 2012).

It has previously been observed that a single sugar unit can act as a switch for a complex-type glycan's three-dimensional structure, thus altering its ligand reactivity and subsequent signaling (Gabius et al., 2011). In the case of a bacterial lectin, the H57A substitution in the cholera toxin B-subunit did not disrupt binding to the GM1 ganglioside, but did lead to loss of immunomodulatory activity and the ability to induce apoptosis, with altered loop position and rigidification affecting further cell surface contacts (Aman et al., 2001). Single nucleotide polymorphisms occur naturally in the genes of human and animal lectins, and these natural sequence changes can affect the carbohydrate recognition domain and biological function, as seen with a human galactose-binding lectin (Ruiz et al., 2014). In this latter case, an impact on cell proliferation and *trans*-interactions has been inferred (Ruiz et al., 2014; Zhang et al., 2015a). Here, we have demonstrated that two distinct properties of a lectin can be separated through rational molecular fine-tuning: BanLec can be engineered to essentially lose its mitogenicity while retaining very potent antiviral activity. The resulting H84T BanLec mutant is a broad-spectrum antiviral agent that is highly active against multiple strains of HCV, influenza, and HIV-1 in tissue culture and *in vivo*; it will also likely prove effective against other clinically important viruses with a suitable presentation of mannose on their surfaces.

Our data suggest that loss of mitogenicity can be achieved by disrupting 83–84 stacking, and disrupting a wall separating two sugar binding pockets, thus diminishing polyvalent interactions. However, doing so while retaining antiviral activity requires a specific amino acid substitution (H84T) that may help retain WT conformational properties as well as possibly form unique contacts that can compensate for loss of interactions with the 83–84 stack. It is possible that these basic design principles can be applied and extended to allow rational engineering of other lectins for use as antiviral tools and other therapeutic purposes. The recent demonstration that *trans*-interactions can be strengthened by insertion of a linker into the homodimer of the antiviral galectin-1 (Zhang et al., 2015b), and the work presented here, encourage such efforts. While the term lectin etymologically stems from the Latin word "legere", meaning to pick, choose, or select (Boyd, 1954), thus emphasizing the natural ability of these proteins to target specific carbohydrates, we have shown that lectins can be made yet more selective through molecular engineering. Our findings also suggest that custom-designed lectins can be employed to tease apart fine mechanisms of immune activation. In more general terms, this proof-of-principle work is likely to inspire the generation of new and innovative tools in the quest to delineate the intricacies of the Sugar Code.

Experimental Procedures

Construction and mutation of BanLec expression vectors, purification of recombinant BanLec mutants

The BanLec cDNA was cloned into a vector allowing for expression of His-tagged protein in *E. coli*, mutagenesis, and purification over a nickel column as described in the Supplemental Experimental Procedures.

Assessment of anti-HIV activity

Assays testing the anti-HIV activity of WT and H84T BanLec in PBMCs were performed as described previously, measuring p24 for HIV-1 and p27 for HIV-2 (Ferir et al., 2011). For the TZM-bl cell assays, to each well of a white 96-well plate 100 μL of a solution containing cells, resuspended at 1×10^5 cells/mL in DMEM medium with 25 mM HEPES and 10% FBS, was added. The next day, the medium was removed by aspiration and fresh medium containing lectin or PBS as a control was added to the plate at a concentration 2-fold higher than the final concentration. After 30 minutes of incubation, virus diluted with medium was added, and the cells were incubated for 48 hours at 37 °C. After the incubation, 100 μL of medium were removed and replaced with 100 μL of ONE-Glo™ Luciferase reagent (Promega) for determination of luciferase expression.

HCV Experiments

The anti-HCV activity of BanLec derivatives was determined for different genotypic chimeras in Huh-7.5 cells using bicistronic *Gaussia* luciferase reporter genomes as described in the Supplemental Experimental Procedures.

Assessment of anti-influenza activity

The *in vitro* anti-influenza activity of H84T, and its efficacy when administered via the intranasal route to female BALB/c mice challenged with influenza, were assessed as described in the Supplemental Experimental Procedures.

Hemagglutination assay and isothermal titration calorimetry (ITC)

Hemagglutination assays conducted using rabbit erythrocytes and ITC were carried out as described in the Supplemental Experimental Procedures

Assessment of mitogenic activity by BrdU incorporation

Mitogenic activity was quantified as is described in the legend for Figure 6 and further in the Supplemental Experimental Procedures.

Flow cytometry to measure cellular activation and Bio-Plex cytokine assay

Expression of CD69 was measured by flow cytometry, and cytokine production following stimulation with lectin by Bio-Plex assay as described in the Supplemental Experimental Procedures.

Vaginal HIV-1 transmission

BLT mice were anesthetized and received 75 μg of H84T BanLec vaginally in a volume of 20 μL. Ten minutes after application of the lectin, the mice were challenged vaginally with 175,000 TCIU of HIV-1 JR-CSF. Mice were bled weekly and the plasma was analyzed for the presence of viral RNA for six weeks as described previously (Wahl et al., 2012).

Glycocluster synthesis and assays

Synthesis of the glycoclusters is described in the Supplemental Experimental Procedures. The determination of the relative ability of glycoclusters to inhibit lectin binding to a matrix presenting a glycoligand, given as the inhibitory concentration (IC) at which the spectrophotometrically-determined signal intensity is reduced by 50% (IC_{50} value), provides a measure of the engagement of a lectin in multivalent associations. This value, and the sensitivity of lectin binding to the surface of cells in culture in the presence of glycoclusters, was assayed as described in the Supplemental Experimental Procedures.

NMR spectroscopy

All NMR experiments were acquired at 313K on a 600 MHz spectrometer equipped with a triple resonance cryoprobe. Y46K/V66D assignment was obtained using a classical 3D assignment strategy. For a more detailed description, see Supplemental Experimental Procedures.

Crystallization, data collection, and structure determination

Following crystallization, data were obtained by LS-CAT and structure, in the presence or absence of dimannoside, was determined as noted in the Supplemental Experimental Procedures

MD Simulations

MD simulations were conducted as described in the Supplemental Experimental Procedures. All simulations were conducted using the Amber 12 package (Case et al., 2005) with the ff99SB*-ILDN force field (Hornak et al., 2006; Lindorff-Larsen et al., 2012). The accelerated MD simulations were set up following the published protocol (Pierce et al., 2012).

Supplementary Material

Refer to Web version on PubMed Central for supplementary material.

Acknowledgments

The authors are grateful to Evelyn Coves-Datson, Anjan Saha, Dana Huskens, Jen Lewis, and Dr. Derek Dube for assistance; Dr. David Smith of LS-CAT for help with remote data collection; and Drs. B. Friday and A. Leddoz for inspiring discussions. Work in the laboratories of D.M.M. and H.M. A-H. was supported by NIH grant 1R01CA14404301. H.-J. G. was supported by the EC-funded GlycoHIT program (contract no. 260600) and Training Network GLYCOPHARM (PITN-GA-2012-317297). M.D.S. and J.V.G. were supported by grants AI096138, AI073146, and P30 AI50410 from the NIH. P.V. M. has been supported by Marie Curie Intra-European Fellowships (500748, 514958, 220948), the Programme for Research in Third-Level Institutions (PRTLI), administered by the Higher Education Authority, the Irish Research Council, Enterprise Ireland and Science Foundation Ireland (04/BR/C0192, 06/RFP/CHO032, 12/IA/1398). R.R. is grateful to the Natural Sciences and

Engineering Research Council of Canada (NSERC) for financial support and for a Canadian Research Chair in Therapeutic Chemistry. The participation of M.A. Papadopoulos and T.C. Shiao are also acknowledged for the preparation of compounds 4–8. M.H.K. received support from the Concerned Parents for AIDS Research. D.S. was supported by KU Leuven grants GOA 10/014 and PF 10/18, European CHAARM grant 242135, and an equipment grant from the Fondation Dormeur, Vaduz. Work in the laboratory of C.M.R was supported in part by PHS grants R01 AI099284, R01 AI072613, and R01 CA057973. Work at Utah State University was supported by Contract Number HHSN2722010000391/HHSN27200005/A37 from the Respiratory Diseases Branch, Division of Microbiology and Infectious Diseases, NIAID, NIH. J.A.S., J.L.M, and H.M. A.-H. were partially supported by P50 GM103297 from the NIH. J.A.S. and J.L.M were also supported in part by the University of Michigan Center for Structural Biology. Use of the Advanced Photon Source was funded by the U. S. Department of Energy under Contract No. DE-AC02-06CH11357, use of the LS-CAT Sector 21 by the Michigan Economic Development Corporation, and the Michigan Technology Tri-Corridor (Grant 085P1000817). Atomic coordinates and structure factors for the reported crystal structure have been deposited within the Protein Data Bank under accession code 3RFP. The PDB codes are 4PIF (wild-type BanLec), 4PIK (wild-type in complex with dimannoside), 4PIT (H84T BanLec mutant), and 4PIU (H84T BanLec mutant in complex with dimannoside). This work is dedicated to the memory of Dr. John Hilfinger, who taught D.M.M. to appreciate biochemistry.

References

Aman AT, Fraser S, Merritt EA, Rodigherio C, Kenny M, Ahn M, Hol WG, Williams NA, Lencer WI, Hirst TR. A mutant cholera toxin B subunit that binds GM1- ganglioside but lacks immunomodulatory or toxic activity. Proc Natl Acad Sci U S A. 2001; 98:8536–8541. [PubMed: 11447291]

André S, Kaltner H, Manning JC, Murphy PV, Gabius HJ. Lectins: getting familiar with translators of the sugar code. Molecules. 2015; 20:1788–1823. [PubMed: 25621423]

Borrebaeck CAK, Carlsson R. Lectins as mitogens. Adv Lectin Res. 1989; 2:10–27.

Boyd, WC. The proteins of immune reactions. In: Neurath, H.; Bailey, K., editors. The Proteins. New York: Academic Press; 1954. p. 756-844.

Case DA, Cheatham TE 3rd, Darden T, Gohlke H, Luo R, Merz KM Jr, Onufriev A, Simmerling C, Wang B, Woods RJ. The Amber biomolecular simulation programs. J Comput Chem. 2005; 26:1668–1688. [PubMed: 16200636]

Ferir G, Vermeire K, Huskens D, Balzarini J, van Damme EJM, Kehr JC, Dittmann E, Swanson MD, Markovitz DM, Schols D. Synergistic in vitro anti-HIV type 1 activity of tenofovir with carbohydrate-binding agents (CBAs). Antiviral Res. 2011; 90:200–204. [PubMed: 21501631]

Gabius HJ, André S, Jiménez-Barbero J, Romero A, Solís D. From lectin structure to functional glycomics: principles of the sugar code. Trends Biochem Sci. 2011; 36:298–313. [PubMed: 21458998]

Gabius HJ. The magic of the sugar code. Trends Biochem Sci. 2015; 40:341. [PubMed: 26006324]

Gabius HJ, Kaltner H, Kopitz J, André S. The glycobiology of the CD system: a dictionary for translating marker designations into glycan/lectin structure and function. Trends Biochem Sci. 2015; 40:360–376. [PubMed: 25981696]

Gavrovic-Jankulovic M, Poulsen K, Brckalo T, Bobic S, Lindner B, Petersen A. A novel recombinantly produced banana lectin isoform is a valuable tool for glycoproteomics and a potent modulator of the proliferation response in CD3+, CD4+, and CD8+ populations of human PBMCs. Int J Biochem Cell Biol. 2008; 40:929–941. [PubMed: 18083059]

Goffard A, Callens N, Bartosch B, Wychowski C, Cosset FL, Montpellier C, Dubuisson J. Role of N-linked glycans in the functions of hepatitis C virus envelope glycoproteins. J Virol. 2005; 79:8400–8409. [PubMed: 15956584]

Hornak V, Abel R, Okur A, Strockbine B, Roitberg A, Simmerling C. Comparison of multiple Amber force fields and development of improved protein backbone parameters. PROTEINS. 2006; 65:712–725. [PubMed: 16981200]

Huskens D, Vermeire K, Vandemeulebroucke E, Balzarini J, Schols D. Safety concerns for the potential use of cyanovirin-N as a microbicidal anti-HIV agent. Int J Biochem Cell Biol. 2008; 40:2802–2814. [PubMed: 18598778]

Khan JM, Qadeer A, Ahmad E, Ashraf R, Bhushan B, Chaturvedi SK, Rabbani G, Khan RH. Monomeric banana lectin at acidic pH overrules conformational stability of its native dimeric form. PLoS One. 2013; 8(4):e62428. [PubMed: 23638080]

Kaltner H, Gabius HJ. A toolbox of lectins for translating the sugar code: the galectin network in phylogenesis and tumors. Histol Histopathol. 2012; 27:397–416. [PubMed: 22374719]

Lindorff-Larsen K, Maragakis P, Piana S, Eastwood MP, Dror RO, Shaw DE. Systematic validation of protein force fields against experimental data. PloS ONE. 2012; 7:e32131. [PubMed: 22384157]

Markwick PR, McCammon JA. Studying functional dynamics in biomolecules using accelerated molecular dynamics. Phys Chem Chem Phys. 2011; 13:20053–20065. [PubMed: 22015376]

Meagher JL, Winter HC, Ezell P, Goldstein IJ, Stuckey JA. Crystal structure of banana lectin reveals a novel second sugar binding site. Glycobiology. 2005; 15:1033–1042. [PubMed: 15944373]

Mo H, Winter HC, van Damme EJ, Peumans WJ, Misaki A, Goldstein IJ. Carbohydrate binding properties of banana (*Musa acuminata*) lectin I. Novel recognition of internal α1,3-linked glucosyl residues. Eur J Biochem. 2001; 268:2609–2615. [PubMed: 11322880]

Murphy PV, André S, Gabius HJ. The third dimension of reading the sugar code by lectins: design of glycoclusters with cyclic scaffolds as tools with the aim to define correlations between spatial presentation and activity. Molecules. 2013; 18:4026–4053. [PubMed: 23558543]

Nakamura-Tsuruta S, Uchiyama N, Peumans WJ, van Damme EJM, Totani K, Ito Y, Hirabayashi J. Analysis of the sugar-binding specificity of mannose-binding-type Jacalin-related lectins by frontal affinity chromatography: an approach to functional classification. FEBS J. 2008; 275:1227–1239. [PubMed: 18266762]

Ng WC, Tate MD, Brooks AG, Reading PC. Soluble host defense lectins in innate immunity to influenza virus. J Biomed Biotechnol. 2012; 2012:e732191.

Palmer AG 3rd. NMR characterization of the dynamics of biomacromolecules. Chem Rev. 2004; 104:3623–3640. [PubMed: 15303831]

Reyes-del Valle J, de la Fuente C, Turner MA, Springfeld C, Apte-Sengupta S, Frenzke ME, Forest A, Whidby J, Marcotrigiano J, Rice CM, et al. Broadly neutralizing immune responses against hepatitis C virus induced by vectored measles viruses and a recombinant envelope protein booster. J Virol. 2012; 86:11558–11566. [PubMed: 22896607]

Ruiz FM, Scholz BA, Buzamet E, Kopitz J, André S, Menendez M, Romero A, Solís D, Gabius HJ. Natural single amino acid polymorphism (F19Y) in human galectin-8: detection of structural alterations and increased growth-regulatory activity on tumor cells. FEBS J. 2014; 281:1446–1464. [PubMed: 24418318]

Sattler M, Schleucher J, Griesinger C. Heteronuclear multidimensional NMR experiments for the structure determination of proteins in solution employing pulsed field gradients. Prog Nucl Mag Res Sp. 1999; 34:93–158.

Singh DD, Saikrishnan K, Kumar P, Surolia A, Sekar K, Vijayan M. Unusual sugar specificity of banana lectin from *Musa paradisiaca* and its probable evolutionary origin. Crystallographic and modelling studies. Glycobiology. 2005; 15:1025–1032. [PubMed: 15958419]

Singh SS, Devi SK, Ng TB. Banana lectin: a brief review. Molecules. 2014; 19:18817–18827. [PubMed: 25407720]

Smee DF, Bailey KW, Wong MH, O'Keefe BR, Gustafson KR, Mishin VP, Gubareva LV. Treatment of influenza A (H1N1) virus infections in mice and ferrets with cyanovirin-N. Antiviral Res. 2008; 80:266–271. [PubMed: 18601954]

Solís D, Bovin NV, Davis AP, Jiménez-Barbero J, Romero A, Roy R, Smetana K Jr, Gabius HJ. A guide into glycosciences: how chemistry, biochemistry and biology cooperate to crack the sugar code. Biochim Biophys Acta. 2015; 1850:186–235. [PubMed: 24685397]

Swanson MD, Winter HC, Goldstein IJ, Markovitz DM. A lectin isolated from bananas is a potent inhibitor of HIV replication. J Biol Chem. 2010; 285:8646–8655. [PubMed: 20080975]

Wahl A, Swanson MD, Nochi T, Olesen R, Denton PW, Chateau M, Garcia JV. Human breast milk and antiretrovirals dramatically reduce oral HIV-1 transmission in BLT humanized mice. PLoS Pathogens. 2012; 8:e1002732. [PubMed: 22737068]

Winter HC, Oscarson S, Slättegård R, Tian M, Goldstein IJ. Banana lectin is unique in its recognition of the reducing unit of 3-O-β-glucosyl/mannosyl disaccharides: a calorimetric study. Glycobiology. 2005; 15:1043–1050. [PubMed: 15888634]

Zhang S, Moussodia RO, Vértesy S, André S, Klein ML, Gabius HJ, Percec V. Unraveling functional significance of natural variations of a human galectin by glycodendrimersomes with

programmable glycan surface. Proc Natl Acad Sci U S A. 2015a; 112:5585–5590. [PubMed: 25902539]

Zhang S, Moussodia RO, Murzeau C, Sun HJ, Klein ML, Vértesy S, André S, Roy R, Gabius HJ, Percec V. Dissecting molecular aspects of cell interactions using glycodendrimersomes with programmable glycan presentation and engineered human lectins. Angew Chem Int Ed. 2015b; 54:4036–4040.

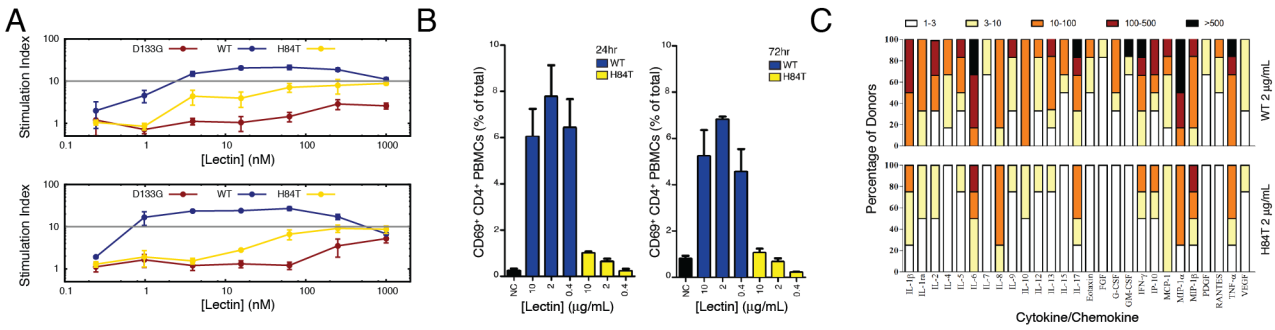

Figure 1. H84T BanLec mutant is significantly less mitogenic than is WT BanLec

(A) Comparisons of the mitogenic activity of H84T to recombinant WT BanLec. PBLs from two different donors were treated with varying concentrations of lectin for three days and then tested for mitogenic activity by measuring BrdU incorporation by ELISA. A stimulation index of less than 10 (grey line) is considered non-mitogenic. The samples for each donor were analyzed in triplicate and error bars represent SEM. The D133G BanLec mutant, in which CBS I is altered (please see Figure 4 below), is not mitogenic but also lacks any antiviral activity (see discussion in text). (B) Induction of the activation marker CD69 on CD4 T cells in the presence of WT or H84T as measured by flow cytometry, one day or three days post-treatment. (C) Induction of cytokines/chemokines by WT and H84T BanLec. PBMCs from healthy donors were incubated for 72 hrs with WT or H84T BanLec at 2 μg/ml. Supernatants were collected and cytokine levels were measured by the Bio-Plex array system. The fold-increase values of the cytokine concentrations in the supernatant of stimulated PBMCs with respect to the concentrations in the supernatant of untreated PBMCs were determined for samples from four different donors. The fold-increase values are divided into subgroups: 1–3 fold-increase (white squares), 3–10 fold-increase (yellow squares), 10–100 fold-increase (orange squares), 100–500 fold-increase (dark red squares), and >500 fold-increase (black squares). See also Figure S1.

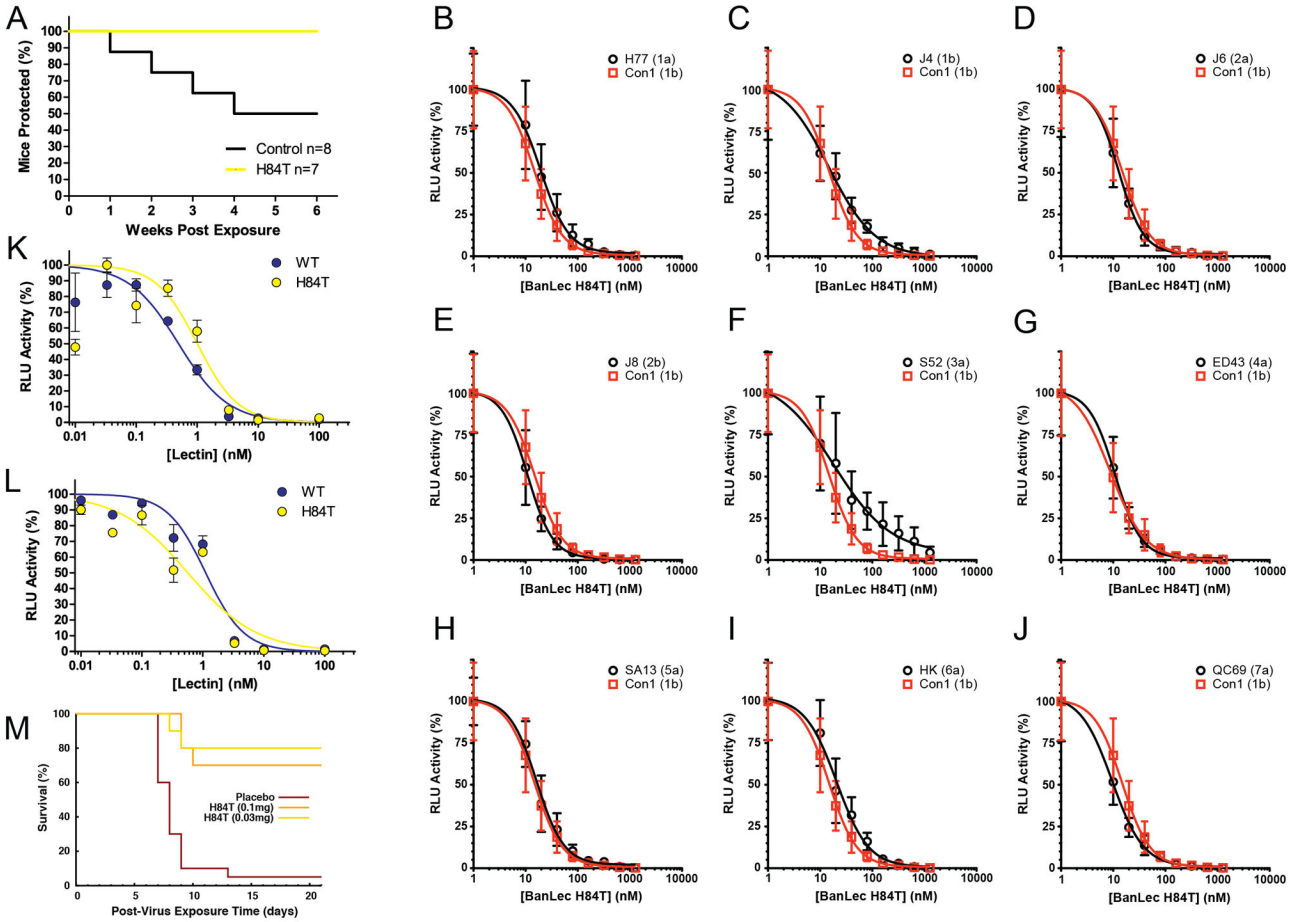

Figure 2. H84T BanLec has potent antiviral activity *in vitro* and *in vivo*

(A) Protection from vaginal HIV-1JR-CSF infection of BLT humanized mice by H84T BanLec. Mice were vaginally exposed to HIV in the presence or absence of topical H84T. HIV infection was determined by the presence of plasma viral load over a period of observation of six weeks. The times to plasma viremia were then combined to generate a Kaplan-Meier plot of the protection from vaginal HIV infection provided by H84T BanLec. Log rank analysis (p=0.0359) confirmed that topically administered H84T prevents vaginal HIV-1 JR-CSF infection in BLT mice. (B–J) Increasing concentrations of H84T (0, 10, 20, 40, 80, 160, 320, 640, 1280 nM) were mixed with the indicated HCVcc inoculum at an MOI 0.1 or 0.05. After 6 h incubation, cells were washed and media containing additional lectin was added. At 72 hours post infection, HCV replication was analyzed by luciferase activity in supernatants. All HCVcc were bicistronic *Gaussia* luciferase reporter genomes of which structural proteins were encoded by differing genotypes as indicated. The means and SD are plotted for two independent experiments containing five replicates each. The corresponding $EC_{50/90}$ values and their respective confidence intervals were determined and are displayed in Table S1. See also Figure S1. (K) The activity of WT or H84T BanLec against the 1918 H1N1 pandemic influenza strain as measured by luciferase assay in the pseudotyped virus system described in the Methods section. (L) The activity of WT and H84T against the H5N1 avian influenza strain as assessed in (K). (M). Survival of mice challenged

intranasally with influenza and then treated with H84T BanLec or control intranasally four hours after challenge and then daily for five days. See also Figure S2 and Table S1.

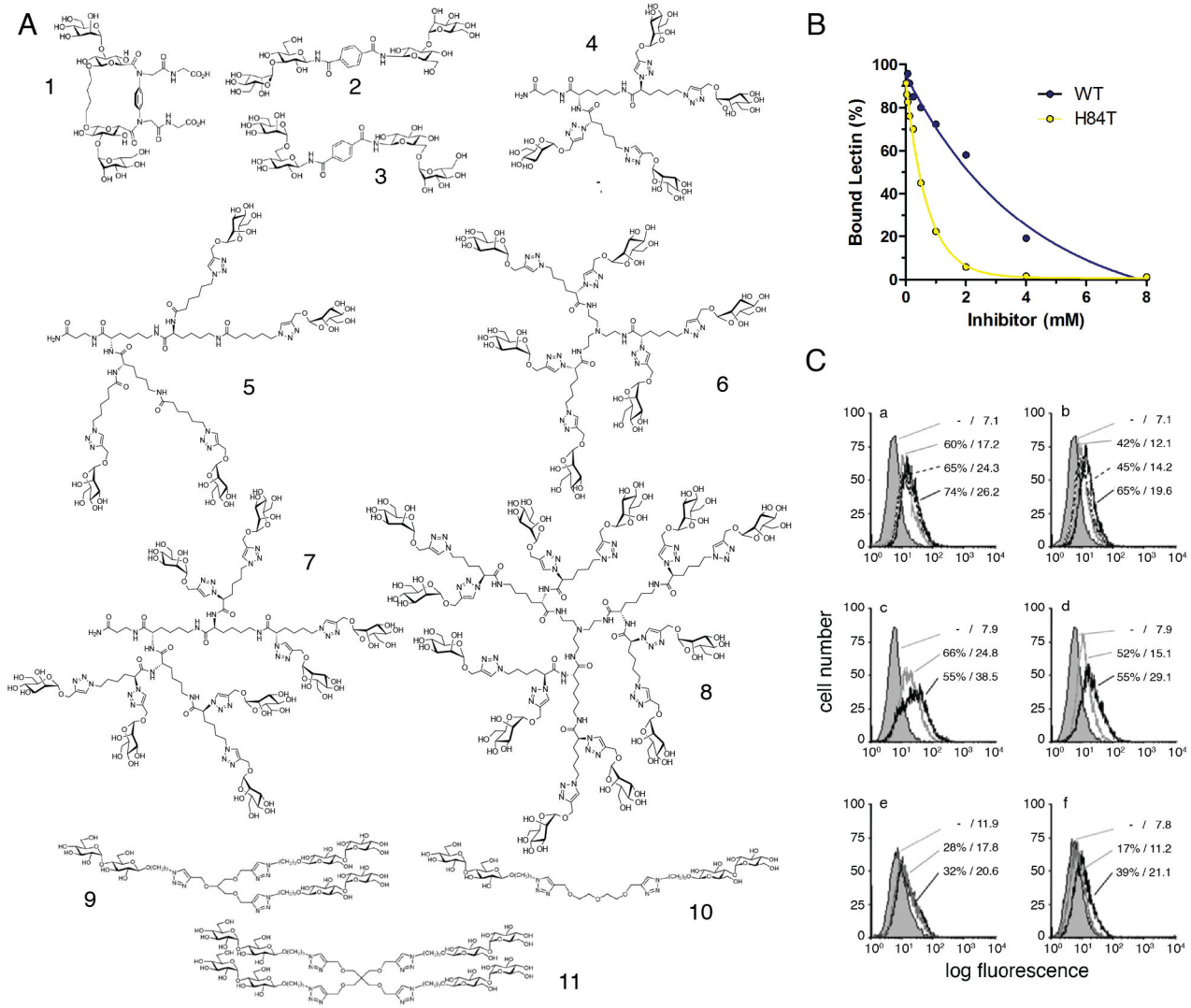

Figure 3. Binding of H84T and WT BanLec to glycoclusters

(A) Structures of the tested glycoclusters. (B) Titration curves for relative signal intensity reflecting extent of binding of the WT (blue) and H84T mutant (yellow) BanLec proteins to surface-immobilized neoglycoprotein in the presence of increasing amounts of the tetravalent maltose-presenting glycocluster (**11**). (C) Semilogarithmic illustration of fluorescent surface staining of human SW480 colon adenocarcinoma cells by labeled WT (left panel) or H84T (right panel) BanLec. Control for background (0%-value) is given as gray area, quantitative data (percentage of positive cells/mean fluorescence intensity) are presented. Lectin staining was monitored with increasing concentrations (1 μg/ml, 2 μg/ml, 5 μg/ml; given in a, b), at 2 μg/ml with cells without (gray) or after treatment (black) with 1-deoxymannojirimycin (c, d) and at 1.5 (WT) or 3 (H84T) μg/ml with the tetravalent glycocluster **11** at 1 mM (WT) or 0.75 mM (H84T) (e, f). See also Tables S2 and S3.

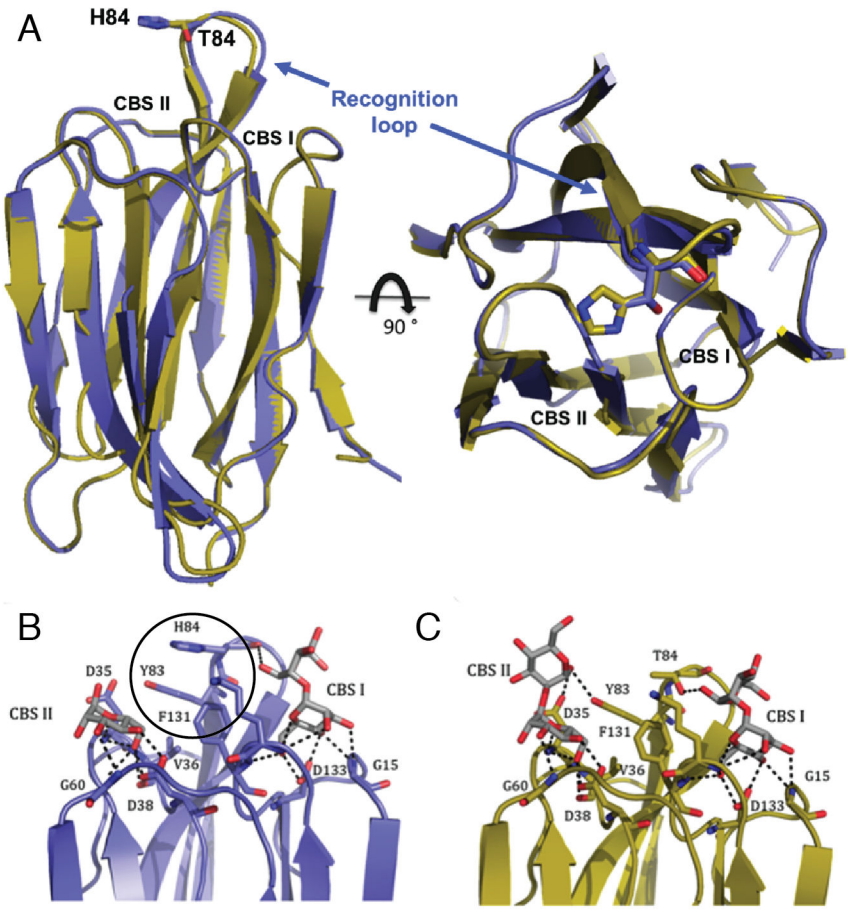

Figure 4. Comparison of crystal structures of recombinant WT BanLec and its H84T mutant

(A) Overlay of the structures of a monomer of recombinant WT (blue) and H84T (yellow) BanLec. Both structures are presented as cartoons with residue 84 shown in ball and stick with oxygen atoms in red, nitrogen atoms in blue, and carbon atoms in the color of the monomer. The N and C termini are labeled. The right image is the result of rotating the left image 90° toward the viewer. CBS=carbohydrate-binding site. (B, C) Binding of a dimannoside to WT BanLec in blue (B) and to the H84T mutant in yellow (C). Disaccharide is shown in gray and individual atoms are colored as in A. Residues involved in hydrogen bonding are shown in ball and stick, and hydrogen bonds are shown as dashed lines. The pipi stacking between Y83 and H84 in the WT protein is circled. See also Figure S3 and Tables S4 and S5.

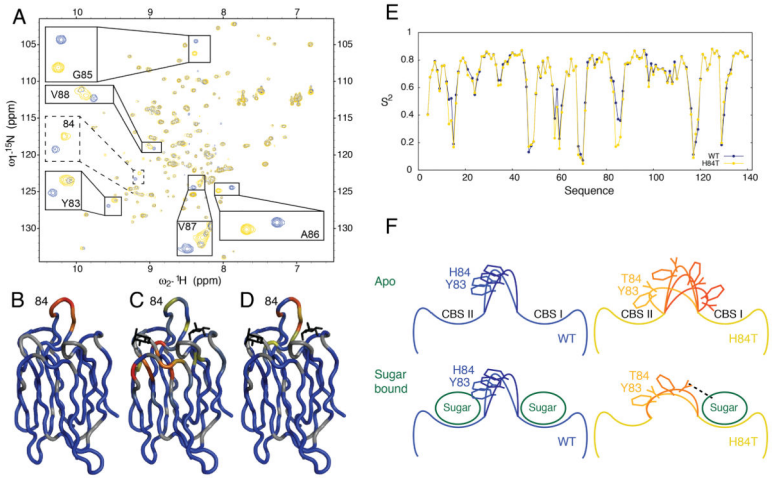

Figure 5. Solution NMR spectroscopy and molecular dynamic simulations reveal dynamic differences in the conformations of WT and H84T BanLec at the third Greek Key

(A) Comparison of H84T mutant and WT BanLec. ^{15}N-^{1}H HSQC spectra of WT (blue) and H84T BanLec (yellow). (B) Chemical shift changes induced by the H84T mutation color-coded on the structure of WT BanLec. (C) Chemical shift changes upon pentamannoside binding color-coded on the structure of WT BanLec. (D) Chemical shift differences between H84T and WT BanLec when interacting with sugar color-coded on the structure of WT BanLec. For B, C and D, the magnitude in chemical shift change increases from blue (no change) to red (maximal change). Gray corresponds to residues for which the change could not be accurately measured. Sugar moieties are in black.

(E). Comparison of WT and H84T Lipari-Szabo order parameters (S^2 varies between 0 and 1 for maximal to minimal flexibility / amplitude of motions, respectively) computed for WT (blue) and H84T (yellow) using accelerated MD. (F). Proposed mechanism for separating antiviral activity and mitogenicity using the H84T mutation. Top: in the apo-form (left), the pi-pi stacking interaction helps separate two binding pockets that can engage with branched N-glycans or sugar moieties on different glycan molecules, creating multivalent interactions, while in the H84T mutant loss of pi-pi stacking between residues 84 and 83 results in a more open binding pocket that can engage multiple sugar moieties on the same glycan molecule, limiting the possibility for multivalent interactions. The dashed line symbolizes the capability of the H84T side-chain to interact with a sugar in the CBS I, which helps to retain the capability to interact with a single sugar while mixing the recognition elements of the two binding sites. See also Figures S4, S5, S6, and S7.

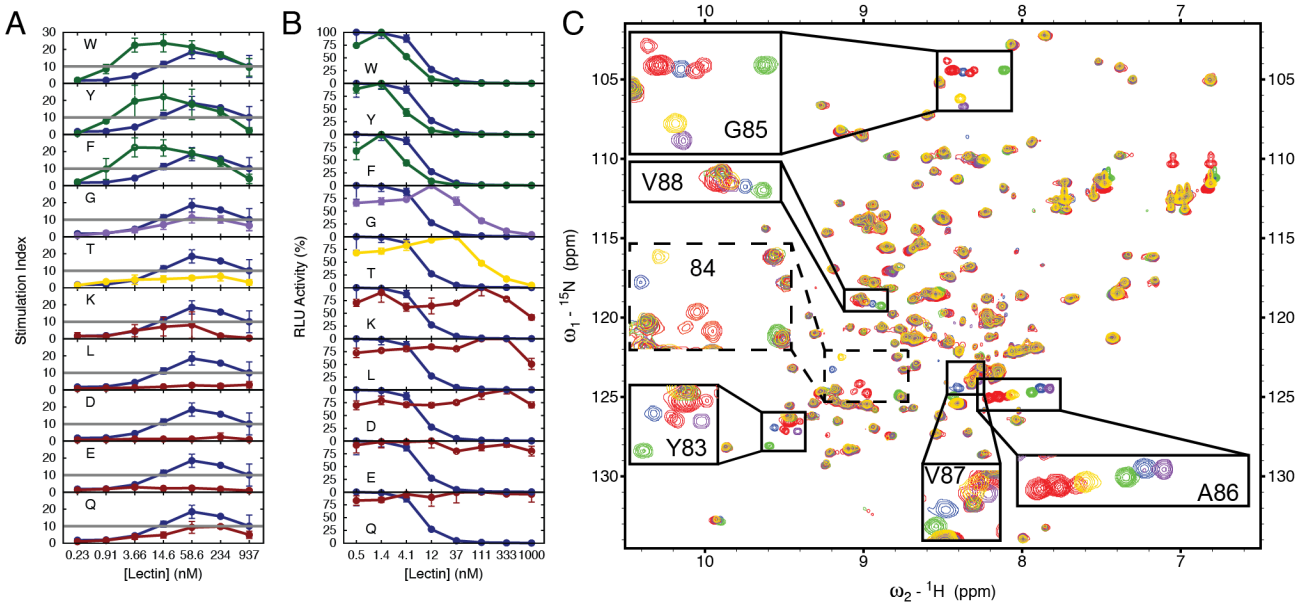

Figure 6. Specific NMR shifts correlate with mitogenicity

(A) Comparison of the mitogenic activity of 10 types of H84X mutants to WT BanLec. PBLs were treated with lectin for three days and tested for mitogenic activity by the incorporation of BrdU reported from an ELISA in relative luminescent units (RLU). A stimulation index (RLU of treated / RLU of untreated) of less than 10 (grey line) is considered non-mitogenic. The type of specific amino acid substitution at position 84 for each mutant is indicated in each figure. Results with WT are plotted in blue for each comparison shown. (B) Antiviral activity of the same BanLec mutants. The anti-HIV activity of each BanLec variant was determined by its ability to block infection of TZM-bl cells with virus pseudotyped with the envelope from the HIV-1 BaL strain. The percentage of relative light unit (RLU) activity with increasing concentrations of lectin is plotted for each H84X mutation.

(C) Comparison of NMR chemical shifts for ten representative H84X mutants of BanLec. ^{15}N-^{1}H HSQCs of WT BanLec and the different mutants. Color coding is as follows: WT BanLec (blue), H84T (yellow), H84G (purple), aromatic mutants H84F, H84W and H84Y (green), and non-aromatic mutants H84D, H84E, H84K, H84Q and H84L (red).

Table 1

Anti-HIV activity profile of BanLec, H84T BanLec, Microvirin (MVN), and the 2G12 monoclonal antibody in PBMCs

	HIV-1								HIV-2
	Lab strain		Group M					Group O	
	NL4.3	BaL	B	C	F	G	H		
			US2	DJ259	BZ163	BCF-DIOUM	BCF-KITA	BCF-06	BV-5061W
	(X4)	(R5)	(R5)	(R5)	(R5)	(R5)	(R5)	(X4)	(X4)
MVN[a]	8	22	2	167	nd	nd	nd	>350	>350
BanLec[a]	0.87	0.87	1.1	2.2	2.5	6.5	3.6	14	3.7
H84T BanLec[a]	2.1	0.93	1.5	0.47	3.1	4.1	1.2	0.73	0.33
2G12mAb[b]	140	3,710	40	>50,000	>20,000	>20,000	>20,000	>20,000	>20,000

[a] 50 % inhibitory concentration (IC_{50}) in nM required to inhibit viral p24 (for HIV-1) or p27 (for HIV-2) production by 50% in PBMCs.

[b] Antibody concentration in ng/ml required to inhibit viral p24 (for HIV-1) or p27 (for HIV-2) production by 50% in PBMCs.

Viral co-receptor usage (R5 or X4) is determined in U87.CD4.CCR5 and U87.CD4.CXCR4 cells and indicated in parentheses.